Journal of Forestry Research (2024) 35:6
https://doi.org/10.1007/s11676-023-01651-0

ORIGINAL PAPER

# Effects of thinning on the understory light environment of different stands and the photosynthetic performance and growth of the reforestation species *Phoebe bournei*

**Shicheng Su[1,2] · Nianqing Jin[1,2] · Xiaoli Wei[1,2]**

Received: 24 November 2022 / Accepted: 13 March 2023


**Abstract** Light levels determine regeneration in stands and a key concern is how to regulate the light environment of different stand types to the requirements of the understory. In this study, we selected three stands typical in south China (a *Cryptomeria japonica* plantation, a *Quercus acutissima* plantation, and a mixed stand of both) and three thinning intensities to determine the best understory light environment for 3-year-old *Phoebe bournei* seedlings. The canopy structure, understory light environment, and photosynthesis and growth indicators were assessed following thinning. Thinning improved canopy structure and understory light availability of each stand; species composition was the reason for differences in the understory light environment. Under the same thinning intensity, the mixed stand had the greatest light radiation and most balanced spectral composition. *P. bournei* photosynthesis and growth were closely related to the light environment; all three stands required heavy thinning to create an effective and sustained understory light environment. In a suitable understory light environment, the efficiency of light interception, absorption, and use by seedlings was enhanced, resulting in a higher carbon assimilation the main limiting factor was stomatal conductance. As a shade-avoidance signal, red/far-red radiation is a critical factor driving changes in photosynthesis and growth of *P. bournei* seedlings, and a reduction increased light absorption and use capacity and height: diameter ratios. The growth advantage transformed from diameter to height, enabling seedlings to access more light. Our findings suggest that the regeneration of shade-tolerant species such as *P. bournei* could be enhanced if a targeted approach to thinning based on stand type was adopted.

**Keywords** Thinning · Understory light environment · *Phoebe bournei* · Photosynthetic performance · Growth performance

## Introduction

Sustainable forest management often uses economically and ecologically valuable tree species to enhance the structure and quality of stands (Schwartz et al. 2015). In the process, the understory light environment has received considerable attention (Cogliastro and Paquette 2012; Gustafsson et al. 2016; Santos and Ferreira 2020) because improving light availability is closely associated with promoting tree growth and stand development and hence, determines future silvicultural benefits (Forrester 2017). Following a comprehensive analysis of the stands' complexity and the ecological strategy of reforestation species, the understory light

Project funding: This study was supported by the National Natural Science Foundation of China (Grant No. 31870613) and Guizhou Province High-level Innovative Talents Training Plan Project (2016) 5661.

The online version is available at http://www.springerlink.com.

Corresponding editor: Yu Lei.

**Supplementary Information** The online version contains supplementary material available at https://doi.org/10.1007/s11676-023-01651-0.

✉ Xiaoli Wei
gdwxl2022@163.com

[1] College of Forestry, Guizhou University, Guiyang 550025, People's Republic of China

[2] Institute for Forest Resources and Environment of Guizhou, Guizhou University, Guiyang 550025, People's Republic of China

Published online: 07 December 2023

environment can be regulated to improve growth to achieve management goals (Daryaei et al. 2019).

The canopy determines the quality of the understory light environment (Forrester et al. 2018; Orman et al. 2021) by intercepting sunlight and thereby directly influencing the radiation intensity and spectral composition that reaches the understory through reflection, transmission, and absorption (Lochhead and Comeau 2012; Schwartz et al. 2015). Crown configuration varies by tree species and the structure of the canopy is determined by the constituent species (Ellsworth and Reich 1993). Canopy structure is a major driver of light diversity during secondary forest succession. For example, successive changes in canopy structure were responsible for changes in light conditions in 14 secondary forest stands in southeastern Mexico (Matsuo et al. 2021). Within a forest stand, there are a wide range of light gradients and understory plants compete for light resources (Ishii et al. 2004; Niinemets 2010; Forrester et al. 2018). Silvicultural measures such as thinning are the simplest, most direct, and most reliable way of changing the canopy structure to provide target species with their optimal light environment and to reduce competition for resources (Beaudet and Messier 2002; Wiener 2010; Santos et al. 2020). Changing light conditions affects the growth and development of plants throughout their life cycle. Furthermore, light requirements and colonization strategies differ among species, therefore any measure that affects light availability should consider both the canopy structure and the ecological needs of the targeted species (Asanok et al. 2013; Giertych et al. 2015). A quantitative understanding of the effects of silvicultural measures on the light environment of different types of forest stands and an analysis of the performance of species in the understory are important for quantifying ecosystem dynamics and the application of forest practices (Dumais et al. 2018; Daryaei et al. 2019). When planting targeted species under different canopies, structure modification to control the light environment should be performed in a specific manner.

The leaf is the most sensitive and adaptable organ with regards to changes in light levels, and several studies have shown that the degree of photosynthetic plasticity can indicate the light requirements of a species (Li et al. 2017; He et al. 2019; Santos and Ferreira 2020). Photons are intercepted, absorbed, and utilized by leaves to complete photosynthesis and assimilate carbon (Dahlgren et al. 2006; Santos and Ferreira 2020). Leaf photosynthetic pathways represent the basic mechanisms by which plants respond to changes in light resources (Poorter and Bongers 2006; Santos et al. 2019). Photosynthesis is driven by captured photons and depends on the wavelength of the absorbed light. Zhen and Bugbee (2020) demonstrated that far-red light (701–750 nm), which accounts for a relatively large proportion of understory light (Zhen et al. 2022), also has significant photosynthetic activity. However, studies on the understory light environment have often only focused on photosynthetically active radiation (400–700 nm) (Oguchi et al. 2006; Wei et al. 2019) and have ignored the importance of far-red light.

*Phoebe bournei* (Hemsl.) Yang is a unique evergreen broadleaf species endemic to China (Wang et al. 2021b). Because *P. bournei* has a tall, straight trunk, and aromatic and durable wood that is dense and lustrous with beautiful patterns (Ge et al. 2014), it is widely used in southern China to transform inefficient secondary forests and restructure pure stands of coniferous trees (Zha et al. 2022). During the early stages of growth, *P. bournei* seedlings exhibit strong shade tolerance and require light-limited conditions for survival and to prevent damage from excessive radiation. However, their light requirements vary with age and hence, *P. bournei* is considered to be rather exacting with regards to light requirements (An et al. 2022). Therefore, when modifying the canopy to meet the light requirements of *P. bournei* growth and development in the understory, a targeted approach is needed, depending on the stand type (Annighöfer 2018; Sendall et al. 2018). To date, little is known about the specific canopy modifications needed to different stands to enhance the understory light environment for the growth and development of *P. bournei.*

Three stand types typical of south China were selected: a *Cryptomeria japonica* (L.f.) D.Don plantation to represent a pure coniferous stand; a *Quercus acutissima* Carruth. plantation as representative of a pure broadleaf stand; and a mixed stand of *C. japonica* and *Q. acutissima* to represent a mixed forest. Three different thinning intensities for each were designed to analyze the effects of thinning on canopy structure and the understory light environment and to investigate the causes of differences in the light environment in the different stands after thinning. In addition, the photosynthetic capacity and growth performance of *P. bournei* planted in the understory was measured to determine its adaptability when the light environment was altered by reducing the canopy cover. The importance of understory far-red light on the growth of *P. bournei* was examined and the hypothesis tested that photosynthetic leaf traits can be used to predict silvicultural effectiveness. Finally, the effects of different stand light environments on the early silvicultural benefits of a *P. bournei* were analyzed to determine how to regulate understory light to optimize the initial growth of *P. bournei* seedlings. This study should provide support for using photosynthetic leaf traits to predict silvicultural effectiveness and help forest managers to regulate the light environment of forest stands.

## Materials and methods

### Study site

This study was conducted in the Bailong Branch of the State-owned Zhazuo Forest Farm (106° 51′–107° 4′ E and 26° 2′–26° 8′ N), Guizhou Province, China, located in a karst basin landscape with a medium-thick loamy soil (Fig. 1). The climate is subtropical humid monsoon with a mean annual temperature of 15.8 °C, a mean annual precipitation of 1213.4 mm, and 282 frost-free days per year. The forest farm is mainly secondary forest because most of the primary vegetation has been removed. The tree species are *C. japonica*, *Q. acutissima*, *Pinus massoniana* Lamb. and *Liquidambar formosana* Hance; shrubs consist of *Rhododendron simsii* Planch. and *Rhus chinensis* Mill.; and herbs are mainly *Pteridium aquilinum* (L.) Kuhn var. *latiusculum* (Desv.) Underw. ex A. Heller and *Miscanthus sinensis* Andersson.

The study was carried out in three stand types: a *C. japonica* plantation (C), a *Q. acutissima* plantation (Q), and a planted mixed stand of *C. japonica* and *Q. acutissima* (M). These stands are at the stage of half-mature forest in the Changshan forest area of the forest farm. Between September and November 2019, an inventory of 10 representative 20 m × 30 m sample plots in each of the three stand types was undertaken (Table 1). Site characteristics (latitude, longitude, altitude, slope and aspect) were determined using GPS and topographic maps (Table 1). The trees in the three stands grew evenly; however, because the stands were mainly composed of one or two species and had a high density, all stands had high canopy closure, weak growth, and a simple hierarchical structure.

### Experimental design

Three thinning intensity levels were carried out: heavy (C1, 59.7%; Q1, 57.3%; M1, 53.7%); moderate (C2, 30.6%; Q2, 26.7%; M2, 28.4%); and light (C3, 0.7%; Q3, 1.3%; M3, 1.5%) for each of the three stands (Table S1), which were determined by the percentage of the stand section area at breast height (SABH) removed by thinning compared with the total SABH of the pre-thinned stand. There were three replicate plots of each thinning intensity level in each of the three stands. Each plot was 400 $m^2$ (20 m × 20 m) with a space of 10 m between plots to avoid adjacent plot interference. At the same time, a 667 $m^2$ plot of bare ground was set as the control (CK). Twenty-eight plots were established (3 stand types × 3 thinning intensity levels × 3 replicate plots + 1 control plot).

At the beginning of March 2020, the free-thinning method was used to harvest trees that were marked according to the experimental design and the actual situation in each plot, giving priority to stressed, dead, and dying trees, while ensuring that a uniform canopy was created as much as possible. All harvest residues and other vegetation in the

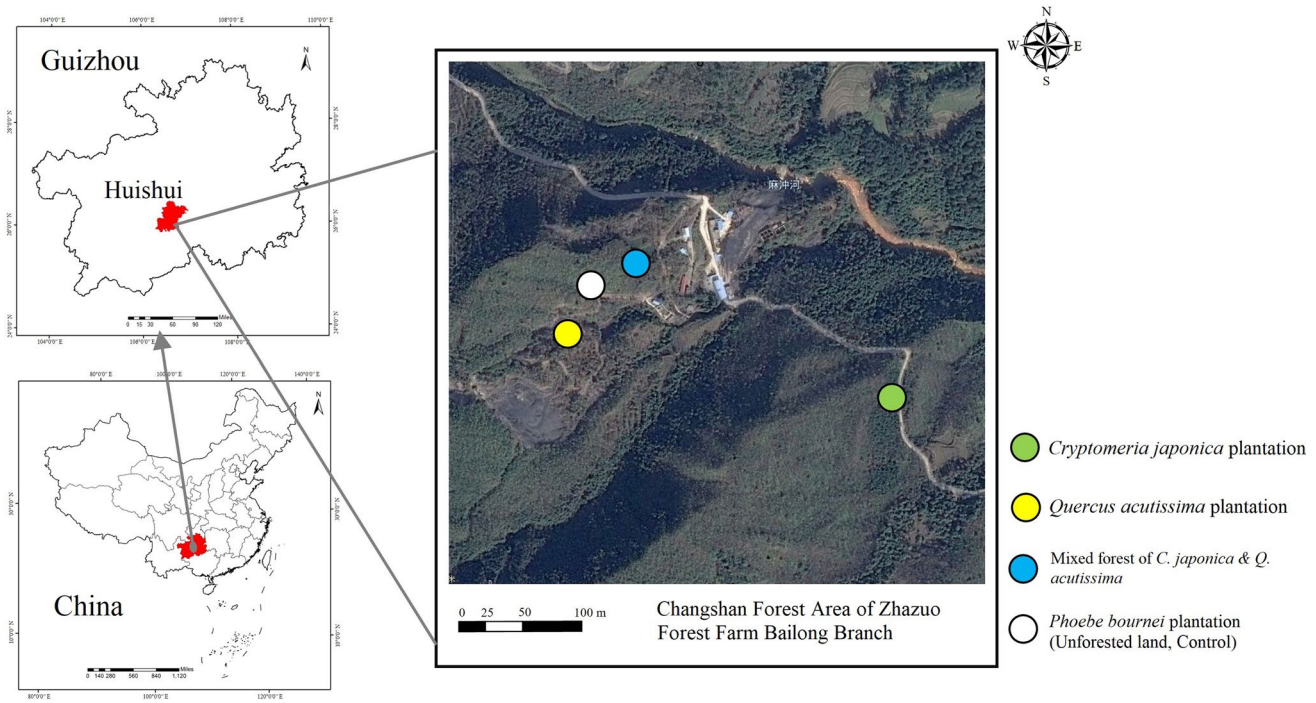


**Fig. 1** Study site location

**Table 1** Characteristics of the stands before thinning

| Stand factor | Longitude | Latitude | m a.s.l | Aspect | Slope | SD (ind. $ha^{-1}$) | CO (%) | ATH (m) | ADBH (cm) | SV ($m^3$ $ha^{-1}$) | TSC |
|---|---|---|---|---|---|---|---|---|---|---|---|
| Stand type | | | | | | | | | | | |
| *C. japonica* plantation (C) | 107° 3′ 57″ E | 26° 6′ 53″ N | 1011.2 | E 90.7° | 5.1° | 1803 ± 162 | 6.7 ± 0.3 | 7.6 ± 0.6 | 10.6 ± 0.7 | 65.4 ± 11.5 | 90% Cj, 10% Qa |
| *Q. acutissima* plantation (Q) | 107° 3′ 37″ E | 26° 6′ 57″ N | 1051.4 | NE 50.6° | 6.9° | 1864 ± 142 | 16.1 ± 0.7 | 7.2 ± 0.7 | 9.5 ± 0.5 | 51.2 ± 9.0 | 90% Qa, 10% Lf |
| Mixed forest (M) | 107° 3′ 42″ E | 26° 7′ 1″ N | 1020.8 | SE 119.6° | 4.3° | 1675 ± 174 | 12.6 ± 0.5 | 7.5 ± 0.8 | 9.7 ± 0.6 | 49.4 ± 11.4 | 50% Cj, 50% Qa |
| Bare ground (CK) | 107° 3′ 40″ E | 26° 6′ 59″ N | 1026.5 | NE 57.6° | 5.8° | – | – | – | – | – | – |

Values = means ± the standard error

*SD* stand density, *CO* canopy openness, *ATH* average tree height, *ADBH* average diameter at breast height, *SV* stocking volume per unit area, *TSC* tree species composition, *Cj Cryptomeria japonica*, *Qa Quercus acutissima*, *Lf Liquidambar formosana*

understory were removed after harvesting to reduce resource competition and to increase the persistence of thinning treatments (Santos et al. 2020). At the end of the month, 36 *P. bournei* seedlings were planted in each replicate plot. Based on previous planting experience with *P. bournei* seedlings and forest inventory results, a spacing of 3 m × 3 m and a planting hole size of 50 cm × 50 cm × 40 cm were used (Fig. S1). A slow-release compound fertilizer (100 g; total nutrients ≥ 45%; A slow-release compound fertilizer (100 g; total nutrients ≥ 45%: 15% N; 15% P; 15% K) was added to each hole as a base fertilizer. In total, 1046 3-year-old *P. bournei* seedlings (height: 48.9 ± 4.5 cm; root collar diameter: 6.5 ± 0.5 mm) were planted (36 seedlings in each of the 27 treatment plots and 74 in the control plot). The seedlings had been cultivated at the experimental nursery at the College of Forestry of Guizhou University (Huaxi, Guiyang) and were marked with red paint at the root collar diameter measurement.

## Canopy structure measurements

Hemispherical photographs of the canopies were obtained and analyzed using WinSCANOPY Pro 2019a (Levelling device: 24MP DSLR Compact OMount; high-resolution camera: SONY ILCE-6000; fish-eye lens; Regent Instruments Inc., Montreal, Quebec, Canada). The center of each plot and the midpoint along a line from the center to the four corners were set as photographing points (Fig. S2) at a camera height of 1.3 m. Three photographs were taken at each of the five photographing points. During the inventory (before thinning, October 2019), 450 hemispherical photographs were taken (i.e., three photographs at each of the five points in ten representative sample plots in each of the stands). In addition, four sets of hemispherical photographs were taken at three (July 2020), six (October 2020), nine (January 2021), and 12 months (April 2021) after thinning in 28 plots (i.e., 15 × 28 = 420 hemispherical photographs × 4 sets = 1680 hemispherical photographs). A total of 2130 hemispherical photographs (450 + 1680) were taken. The photographs were taken in the morning (07:00–08:00 am) or in the afternoon (17:00–18:00 pm) on cloudy, windless days to ensure consistent light conditions and to minimize halos caused by direct light. When the hemispherical photographs were analyzed, information (latitude, longitude, m above sea level, slope and aspect) relating to each photographing point was entered (Fig. S3). The stand canopy status in each plot was determined using the mean values of the hemispherical photograph analysis data. Canopy openness (CO) and leaf area index (LAI) were used to characterize the canopy structure, and the under-canopy photosynthetic photon flux density (UPPFD, including direct and diffuse radiation) was used to characterize the understory light conditions.

### Spectral measurements above the crown of *P. bournei* seedlings

Spectral measurements were conducted using a high-sensitivity spectrometer (cosine corrector: CC-3; fiber: QP400-2-VIS–NIR; software: Oceanview 1.6.3 and MAYA2000, Ocean Optics Inc., Dunedin, FL, USA) from 11:00–14:00 h on consecutive, sunny days. Measurements were recorded at three (July 2020), six (October 2020), nine (January 2021), and twelve months (April 2021) after planting the seedlings. Eighteen *P. bournei* seedlings were selected in each plot (uniformly distributed within the plots, Fig. S1). The cosine corrector was placed 5 cm above their crowns and spectral measurements of the following waveband data were recorded once every 15 s for a total of three times: red radiation (R, 655–665 nm), far-red radiation (FR, 725–735 nm), wideband red radiation (Rw, 600–700 nm), and wideband blue radiation (Bw, 400–500 nm). R/FR and Rw/Bw ratios were calculated.

### Photosynthetic leaf trait measurements

Every three months (July 2020, October 2020, January 2021 and April 2021) after planting, five average plants were selected from each plot, and photosynthetic traits (light interception, absorption, use, and gas exchange characteristics) of peripheral leaves on the second or third branches down from the top of the crowns were measured. Leaves used for measurements were fresh, pest-free, and fully developed. When the first light-use and gas-exchange characteristics were measured, leaves were marked with a label.

### Light interception: specific leaf area (SLA)

Three leaves were cut from each sample plant and a 1-$cm^2$ area cut from each leaf, which were oven-dried at 105 °C for 0.5 h and then at 75 °C for 48 h until a constant weight was reached. The SLA was determined by calculating the leaf area ($cm^2$): dry mass (g) ratio.

### Light absorption: chlorophyll *a* and *b* ratio ($Chl_{a/b}$) and total chlorophyll content ($Chl_{total}$)

Three fresh leaves were cut from each sample plant to determine photosynthetic pigments: 0.1 g of fresh leaves of each sample plant were placed in a graduated test tube, 10 ml of 95% ethanol added and the tube then placed in the dark for 48 h until the leaves turned white. After filtration, chlorophyll *a* and chlorophyll *b* absorbance readings were taken at two wavelengths (663 and 645 nm) using a UV-2100 spectrophotometer (Unico, Dayton, NJ, USA). $Chl_{a/b}$ and $Chl_{total}$ concentrations in the extracts were calculated based on the content of chlorophyll *a* and chlorophyll *b* (mg $g^{-1}$) (Lichtenthaler and Wellburn 1983).

### Light use: maximum quantum yield of photosystem II (PSII), $F_v/F_m$; actual quantum yield of PSII, Y(II)

Light use measurements were carried out on three leaves of each plant using a MONI-PAM fluorometer (Heinz Walz GmbH, Effeltrich, Germany) after dark adaptation for 0.5 h and avoiding the main veins of the leaves. The $F_v/F_m$ value was calculated by determining the initial fluorescence value ($F_o$) using an irradiation measurement light (< 0.5 µmol $m^{-2}$ $s^{-1}$), and the maximum fluorescence value ($F_m$) was determined using a 0.6 s saturation pulse (approximately 10,000 µmol $m^{-2}$ $s^{-1}$) (Tsimilli-Michael and Strasser 2008; Strasser et al. 2010).

### Gas exchange characteristics: light-saturated photosynthesis rate ($A_{sat}$) and stomatal conductance ($g_s$)

Three leaves per plant were measured using a portable gas exchange analyzer (LI-6800, Li-Cor Inc., Lincoln, NE, USA) between 09:00 and 11:00 am on typical, consecutive sunny days. The chamber was adjusted to the following parameters: a flow rate of 400 µmol $m^{-2}$ $s^{-1}$, a $CO_2$ concentration of 400 µmol $mol^{-1}$, a leaf temperature of 25 °C, and a photosynthetic photon flux density of 1500 µmol $m^{-2}$ $s^{-1}$.

### Seedling growth measurements

Every three months after planting, height (H, cm), root collar diameter (D, mm), and crown radii (cm) of all seedlings were measured. The crown area (CA, $cm^2$) was calculated using Eq. 1:

$$CA = \pi * A * B/4 \quad (1)$$

where *A* and *B* are the lengths of the long and short axes of the crowns, respectively. The approximate aboveground seedling biomass was calculated by determining $HD^2$ (Kohyama and Hotta 1990). The annual relative growth rate (RG) of the aboveground biomass was calculated using Eq. 2:

$$RG = \ln HD_1^2 - \ln HD_0^2 \quad (2)$$

where $HD_0^2$ is the plant biomass on the day of planting and $HD_1^2$ is the biomass one year after planting (April 2021) (Santos and Ferreira 2020).

### Statistical analysis

Microsoft Excel 2021 was used for preliminary data organization and statistical analyses performed in SPSS 26.0.

One-way ANOVA was used to test statistical differences among treatments, and Tukey's test was used for post-hoc analysis ($P < 0.05$). The Spearman correlation method was used to preliminarily analyze the correlations of all indicators. Path analysis was used to study the correlation structure between the independent variable $X_i$ ($i = 1, 2, \ldots, n$) and the dependent variable $Y$ (Silveira et al. 2015; Wang et al. 2021a) to distinguish the effects of $X_i$ on $Y$ into direct and indirect effects after obtaining the optimal regression equation using stepwise regression analysis, and to judge the relative importance of the contributions of the respective variables to the dependent variable by determining the magnitude of the path coefficients (Fig. 2).

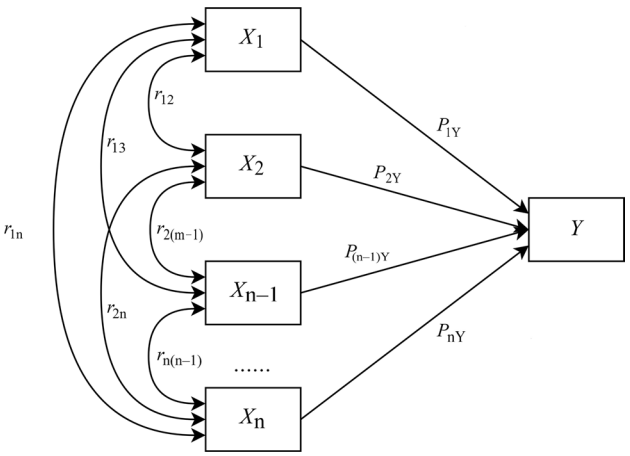


**Fig. 2** Graph of path analysis; double-headed arrows indicate the indirect effect of $X_i$ on $Y$ via the $X_j$ correlation path (*rij*, indirect determination coefficient); single-headed arrows indicate the direct effect of $X_i$ on $Y$ (*PnY*, direct determination coefficient)

## Results

### Canopy structure and understory light environment

With greater thinning intensity, CO (canopy opening) and UPPFD (under canopy photosynthetic photon flux density) increased significantly, and LAI (leaf area index) decreased significantly in the three stands (Fig. 3). At the same thinning intensity, CO was greatest in the *Q. acutissima* plantation and smallest in the *C. japonica* plantation, with the CO of the *Q. acutissima* plantation 1.4, 2.2 and 2.2 times greater following light, moderate, or heavy thinning, respectively. The regrowth of canopies resulted in a reduction in CO over time, with the *Q. acutissima* plantation showing the greatest reduction (i.e., a reduction 3.8 times greater than that of the *C. japonica* plantation, which showed the smallest reduction). *Q. acutissima* is a deciduous species, therefore the CO of the plantation and mixed stand increased rapidly in January (winter). The LAI of each stand showed the opposite to that observed for CO.

Comparisons of UPPFD in different stands that received the same thinning revealed that the mixed stand had the highest value (Fig. 3). Canopy structure of the species differed and hence the proportion of each radiation component reaching the understory was different. Direct radiation in the *C. japonica* plantation was relatively high, comprising 92.0% of the UPPFD, whereas diffuse radiation in the *Q. acutissima* plantation was 12.3% of the UPPFD. The *C.*

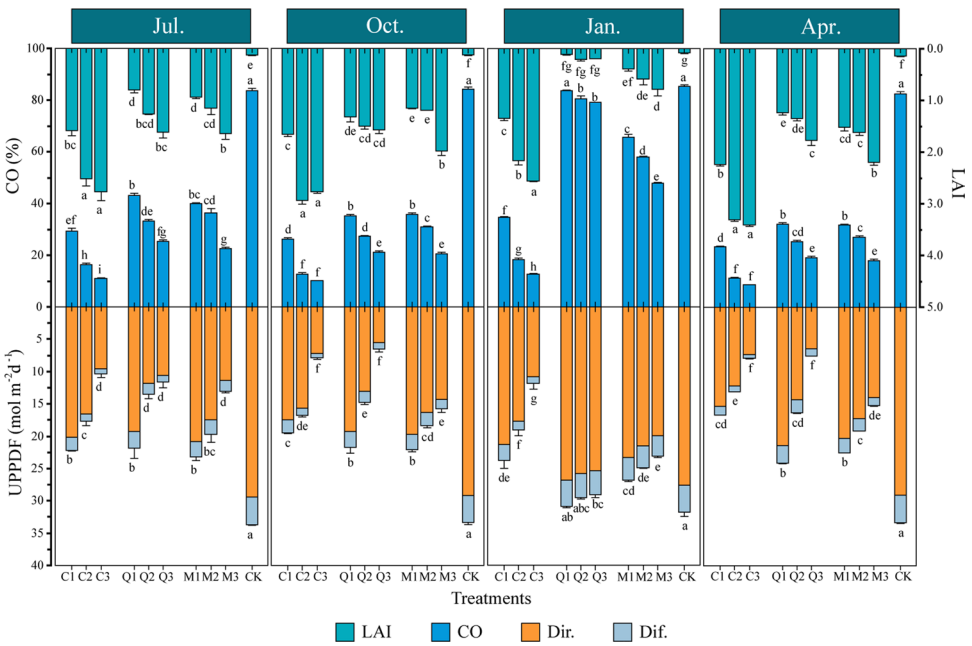


**Fig. 3** Effects of three thinning intensities (1, heavy; 2, moderate; 3, light) on CO, LAI, and UPPFD in three forest stands (C, *Cryptomeria japonica*; Q, *Quercus acutissima*; M, mixed forest of *C. japonica* and *Q. acutissima*; and CK, bare ground control) over time. Bars indicate means and error bars indicate the total standard error. Different letters in the same month indicate significant differences between treatments ($P < 0.05$) according to Tukey's test. Abbreviations: CO, canopy openness; LAI, leaf area index; UPPFD, under-canopy photosynthetic photon flux density (Dir., direct radiation; Dif., diffuse radiation)

*japonica* plantation showed an average decrease in UPPFD of 25.1% over time under all three thinning regimes. In contrast, there was little change in UPPFD over time in the mixed stand.

### Spectra above the crown of *P. bournei* seedlings

The spectra above the crowns of *P. bournei* seedlings in the different stands after different thinning intensities showed significant differences (Table 2). The greater the CO, the higher the radiation in each wavelength, and R/FR and Rw/Bw were also significantly higher. Except in January, R/FR and Rw/Bw decreased over time in each stand, with the maximum R/FR in plots of heavily thinned *C. japonica* and the minimum in plots of *C. japonica* subjected to moderate or light thinning. The opposite situation was recorded in the mixed stand, with the R/FR of *C. japonica* plots 1.1, 0.9, and 0.9 times higher than those in mixed stands subjected to heavy, moderate, or light thinning, respectively. Rw/Bw did not differ significantly among heavily thinned stands; however, Rw/Bw was lowest in the *C. japonica* plantation subjected to moderate or light thinning and the maximum was in the *Q. acutissima* plantation, about 1.1 times that of the *C. japonica* plantation. Following thinning, the *C. japonica* plantation showed the greatest variation in R/FR and Rw/Bw among the three stands, and the understory spectral composition was the most strongly influenced by thinning.

### Photosynthetic leaf traits

The photosynthetic leaf traits of *P. bournei* seedlings differed significantly in response to different thinning (Fig. 4). Over time, SLA, $Chl_{total}$, $F_v/F_m$, and Y(II) decreased trend with increasing CO (Fig. 4a, b, d, e), and $Chl_{a/b}$ increased with increasing CO (Fig. 4c). However, $g_s$ (Fig. 4f) and $A_{sat}$ (Fig. 4g) both increased and then decreased with greater CO in July, and increased with greater CO in April. Control seedlings had relatively small photosynthetic leaf trait values except for the $Chl_{a/b}$, which was significantly larger than that of seedlings grown under stands.

### Height, root collar diameter, and crown growth

Increments in height and root collar diameter of *P. bournei* seedlings in stands subjected to different thinning treatments varied significantly (Fig. 5) because of changes to the canopy structure and in the understory light environment. With greater thinning intensity, increment of root collar diameter in all three stands showed an increasing trend, however, increment of height only showed an increasing trend in the *C. japonica* plantation, and increased then decreasing trend in the *Q. acutissima* plantation and mixed stand. Increments in root collar diameter were highest in the mixed stand and lowest in the *C. japonica* plantation for all three thinning treatments. Of the stands subjected to heavy thinning, seedlings in the *C. japonica* plots showed the largest height increment, and among stands under moderate or light thinning, *P. bournei* seedlings in the mixed stand showed the largest height increment. Control seedlings in full sunlight performed poorly, with height and root collar diameter increments that were 46.2% and 74.4% of the best-performing treatments (M2 and M1), respectively.

Crowns of *P. bournei* seedlings in the understory of the different stands gradually diversified over time (Table 3). After 12 months, crowns of seedlings in the *C. japonica* plantation had grown larger with increasing thinning intensity. However, seedlings in the *Q. acutissima* plantation and mixed stand showed a significantly greater crown area under moderate thinning. The RG (relative growth rate) of seedlings increased with greater thinning intensity, with the maximum for seedlings planted in heavily thinned mixed forest (M1), relatively minor for seedlings in full sunlight (CK), and minimum for seedlings in *C. japonica* plots subjected to light thinning (C3). The RG of M1 was 2.5 and 1.3 times more than C3 and the controls, respectively.

### Correlation between stand canopy structure, understory light environment and photosynthetic leaf traits and growth

Correlations between all indicators were studied using the Spearman correlation method (Fig. 6). Canopy structure (opening and leaf area index) significantly influenced understory light conditions, and CO was positively correlated with UPPFD, R/FR, and Rw/Bw ($P < 0.01$) and negatively with LAI ($P < 0.01$). Photosynthetic leaf traits of light interception (SLA), absorption ($Chl_{a/b}$, $Chl_{total}$), and use (Y(II), $F_v/F_m$) were correlated with the light environment ($P < 0.01$). $g_s$ was positively correlated with UPPFD ($P < 0.05$) and was positively correlated with R/FR and Rw/Bw ($P < 0.01$). RG was significantly correlated with all light environment factors and with seedling photosynthetic and growth indicators ($P < 0.01$), whereas height growth was correlated only with photosynthetic traits and not with the light environment. Root collar growth showed no correlation with light availability; however, crown growth was positively correlated with the understory light environment but not with canopy structure (CO and LAI). However, the correlation coefficient does not fully explain the relationship between the environment and seedling performance. For example, $A_{sat}$ is the most critical indicator representing the rate of carbon assimilation which is directly influenced by light. However, $A_{sat}$ was not significantly correlated with the light environment in the correlation analysis. This suggests that the correlation coefficient ignores the relative

**Table 2** Changes in spectral composition above the crown of *P. bournei* seedlings among thinning treatments over time

| Spectrum | Treatments | R/FR | Rw/Bw |
|---|---|---|---|
| 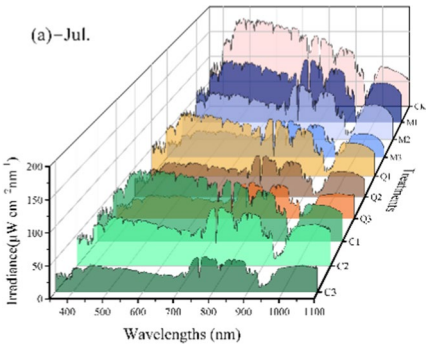 | C1 | 1.27 ± 0.003 [b] | 0.99 ± 0.006 [b] |
| | C2 | 0.93 ± 0.009 [e] | 0.86 ± 0.003 [d] |
| | C3 | 0.79 ± 0.004 [g] | 0.77 ± 0.007 [f] |
| | Q1 | 1.23 ± 0.010 [c] | 0.99 ± 0.008 [b] |
| | Q2 | 1.01 ± 0.008 [d] | 0.95 ± 0.007 [c] |
| | Q3 | 0.86 ± 0.010 [f] | 0.87 ± 0.005 [d] |
| | M1 | 1.20 ± 0.007 [c] | 0.98 ± 0.006 [b] |
| | M2 | 1.03 ± 0.006 [d] | 0.89 ± 0.009 [d] |
| | M3 | 0.90 ± 0.008 [e] | 0.81 ± 0.002 [e] |
| | CK | 1.35 ± 0.007 [a] | 1.07 ± 0.004 [a] |
| 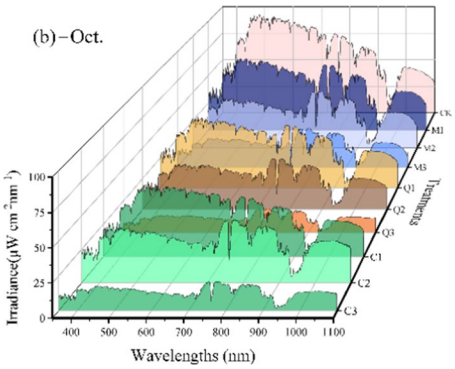 | C1 | 1.26 ± 0.001 [ab] | 0.99 ± 0.003 [b] |
| | C2 | 0.91 ± 0.010 [d] | 0.85 ± 0.002 [de] |
| | C3 | 0.75 ± 0.021 [e] | 0.76 ± 0.021 [f] |
| | Q1 | 1.20 ± 0.003 [b] | 0.96 ± 0.007 [bc] |
| | Q2 | 1.01 ± 0.045 [c] | 0.93 ± 0.012 [c] |
| | Q3 | 0.88 ± 0.013 [d] | 0.86 ± 0.003 [d] |
| | M1 | 1.20 ± 0.006 [b] | 0.94 ± 0.007 [c] |
| | M2 | 1.01 ± 0.015 [c] | 0.86 ± 0.007 [d] |
| | M3 | 0.89 ± 0.012 [d] | 0.81 ± 0.002 [e] |
| | CK | 1.35 ± 0.004 [a] | 1.06 ± 0.004 [a] |
| 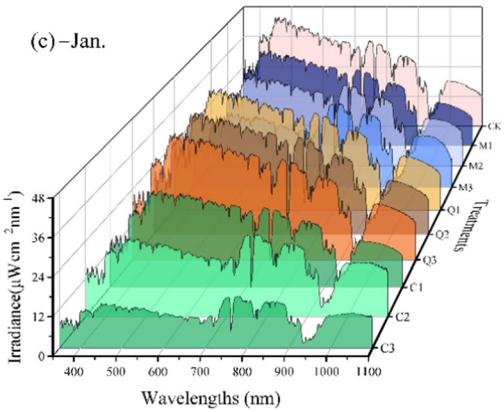 | C1 | 1.27 ± 0.002 [c] | 1.01 ± 0.007 [bc] |
| | C2 | 0.95 ± 0.002 [e] | 0.84 ± 0.004 [e] |
| | C3 | 0.81 ± 0.004 [f] | 0.77 ± 0.009 [f] |
| | Q1 | 1.32 ± 0.002 [ab] | 1.03 ± 0.003 [ab] |
| | Q2 | 1.32 ± 0.004 [ab] | 1.02 ± 0.005 [abc] |
| | Q3 | 1.31 ± 0.003 [ab] | 1.01 ± 0.008 [abc] |
| | M1 | 1.30 ± 0.004 [bc] | 1.00 ± 0.008 [c] |
| | M2 | 1.22 ± 0.017 [d] | 0.92 ± 0.009 [d] |
| | M3 | 0.94 ± 0.006 [e] | 0.88 ± 0.009 [e] |
| | CK | 1.34 ± 0.006 [a] | 1.04 ± 0.004 [a] |
| 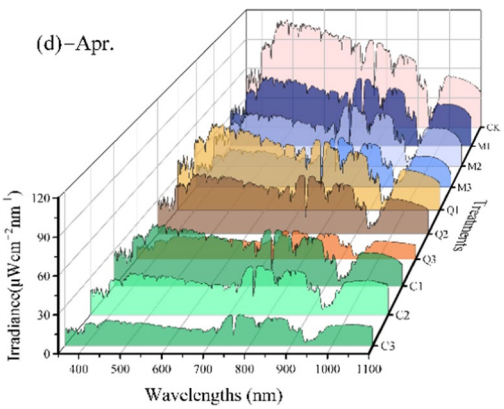 | C1 | 1.25 ± 0.007 [b] | 0.99 ± 0.008 [b] |
| | C2 | 0.90 ± 0.007 [e] | 0.84 ± 0.005 [ef] |
| | C3 | 0.75 ± 0.005 [f] | 0.74 ± 0.011 [g] |
| | Q1 | 1.20 ± 0.005 [b] | 0.94 ± 0.011 [c] |
| | Q2 | 1.01 ± 0.025 [d] | 0.90 ± 0.003 [cd] |
| | Q3 | 0.86 ± 0.006 [e] | 0.84 ± 0.006 [ef] |
| | M1 | 1.14 ± 0.012 [c] | 0.92 ± 0.006 [c] |
| | M2 | 1.01 ± 0.014 [d] | 0.87 ± 0.007 [de] |
| | M3 | 0.87 ± 0.004 [e] | 0.81 ± 0.003 [f] |
| | CK | 1.37 ± 0.010 [a] | 1.06 ± 0.009 [a] |

**Table 2** (continued)

Treatments: stands of *Cryptomeria japonica* (C), *Quercus acutissima* (Q), mixed forest of *C. japonica* and *Q. acutissima* (M), and bare ground control (CK) were subjected to heavy (1), moderate (2), or light (3) thinning prior to planting *P. bournei* seedlings in the understory. Values represent means ± standard error. Different letters in the same month indicate significant differences among treatments ($P < 0.05$). R/FR, red/far-red radiation ratio; Rw/Bw, wideband red/wideband blue radiation ratio

importance between variables, therefore, the relationship between indicators needs to be further analyzed.

### Path analysis

The direct effects of independent variables on dependent variables and the indirect effects of interactions between these were examined in detail using stepwise regression and path analyses to identify essential links between several independent and dependent variables to provide a reliable basis for statistical decision-making (Wang et al. 2021a). Figure 7a and b show that CO, LAI, and R/FR in the light environment have a limiting effect on the $A_{sat}$ of *P. bournei* seedlings, and that CO is the main limiting factor with the strongest direct effect according to the order of determination coefficients. All indicators of the leaf photosynthetic pathway play a role in enhancing $A_{sat}$, among which $g_s$ is the main decision variable and has the strongest direct effect. With regard to variables affecting seedling growth (Fig. 7c, d), light environment variables that enhanced RG were LAI, Dif., and R/FR, while CO and Rw/Bw were limiting factors, CO had the greatest direct effect on growth, followed by Dif. Among the leaf photosynthetic pathways, only SLA and $g_s$ were retained after stepwise regression, with both of these enhancing seedling growths. SLA was the main decision variable with the largest direct effect on seedling growth. Our analyses show that if the canopy is too open (strong light) or if the LAI is too high (excessive shade), the carbon assimilation rate of *P. bournei* seedlings can be inhibited. Therefore, *P. bournei* seedlings need both a suitable stand canopy structure and an understory light environment for growth and development. Furthermore, both $A_{sat}$ and RG are influenced by R/FR, with R/FR also playing a major role in determining RG.

## Discussion

### Effect of thinning on canopy structure and understory light environments

Different stands have different canopy structures and light environments (Gustafsson et al. 2016; Orman et al. 2021). Thinning creates special microenvironments in the understory by changing the canopy structure. The most direct effect is to increase light availability in the understory (Santos et al. 2020). Thinning modified the canopy structure and the understory light environment of the three stands by reducing stand density, making the canopy sparse (Beaudet et al. 2011; Zhang et al. 2018a). CO and understory radiation significantly increased, and LAI decreased in all stands with increasing thinning (Fig. 3 and Table 2). However, the thinning measures had different effects on canopy structure and light conditions of the different stands. For example, the same thinning intensity had a greater effect on canopy structure of stands with a greater proportion of broadleaf trees. After thinning, the canopy opening of the *C. japonica* plantation, mixed species stand, and the *Q. acutissima* plantation ranged from 11.0 to 29.4%, 22.6 to 39.9%, and 25.3 to 43.0%, respectively (Fig. 3). Over time, canopies closed. However, the rate of closure varied with species composition and thinning intensity determining the speed of closure (Forrester et al. 2018; Santos et al. 2020). Although canopies of *Q. acutissima* plots under heavy thinning closed more rapidly after thinning than canopies in other plots, the understory radiation of these *Q. acutissima* plots decreased more slowly. Twelve months after thinning, the UPPFD in the *C. japonica* plantation had decreased the most, averaging about 25.1%, whereas in the *Q. acutissima* plantation, it had only decreased by 1.5% (Fig. 3). When the three stands were subjected to the same thinning intensity, Dir. was highest in the *C. japonica* plantation and Dif. highest in the *Q. acutissima* plantation, whereas the proportion of Dir. and Dif. in the mixed stand was more balanced and had the highest radiation. This indicates that, when the three stands were subjected to the same thinning intensity, the light environment of the mixed forest improved more effectively, which is consistent with the findings of previous studies that investigated the effect of canopy structure on forest light environment (Ishii et al. 2004; Beaudet et al. 2011; Forrester et al. 2018).

Several studies have investigated how to assess the understory light environment effectively (Cogliastro and Paquette 2012; Lochhead and Comeau 2012; Rosati et al. 2013). In this study, factors associated with canopy structure were closely related to the understory light environment, and the combined effects of the canopy opening and leaf area index of the three stands affected radiation intensity and spectral composition (Fig. 6). Therefore, light conditions in a stand can be effectively estimated by measuring CO and LAI. These measurements, combined with radiation intensity and the spectral composition of the understory, can then be used to analyze and evaluate the light environment in the stand (Orman et al. 2021). Blue, red, and far-red light in the spectrum play key roles in controlling the photomorphogenesis,

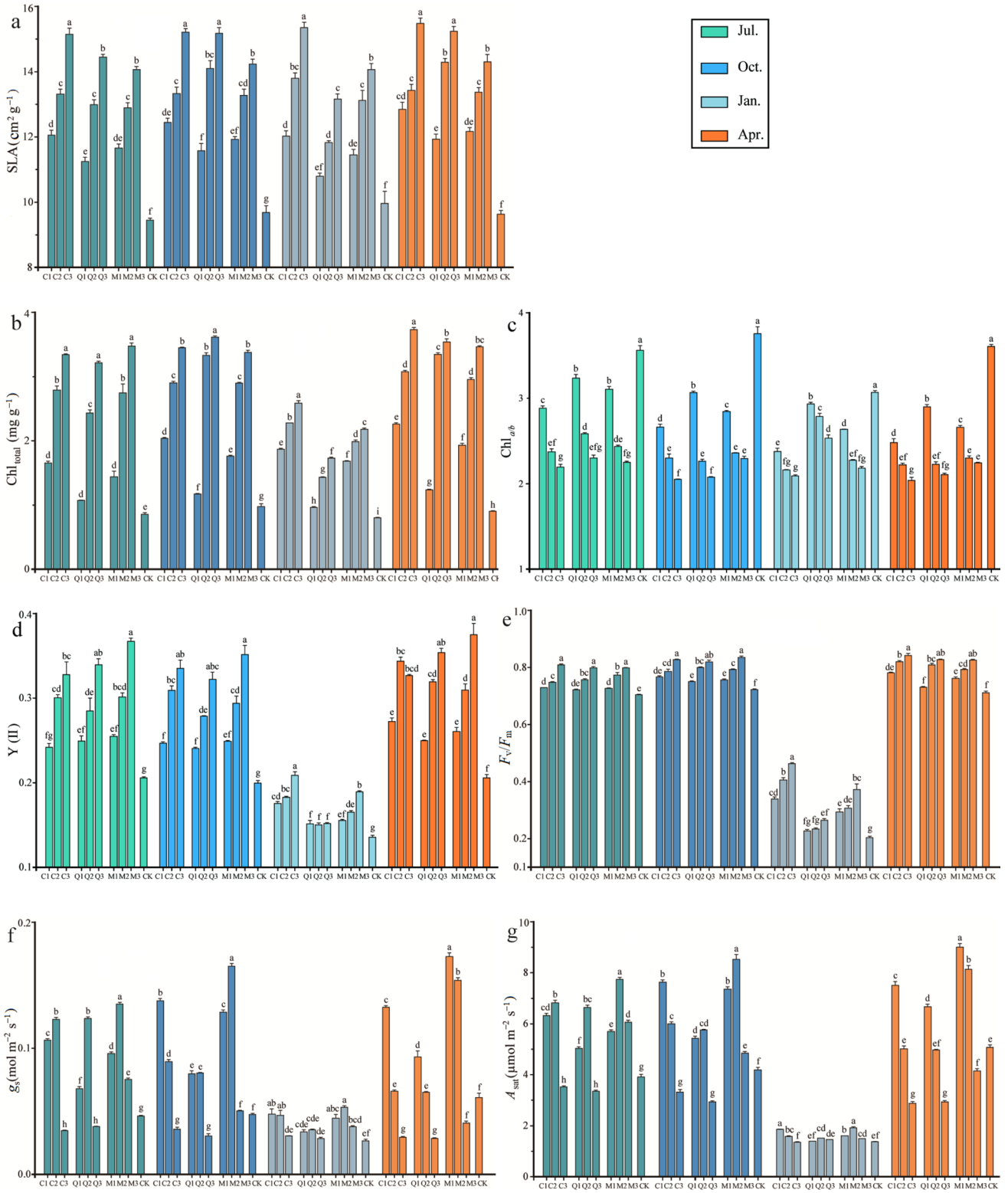


**Fig. 4** Leaf photosynthetic trait response over time of *P. bournei* seedlings planted in three stands [*Cryptomeria japonica* (C), *Quercus acutissima* (Q), mixed forest of *C. japonica* and *Q. acutissima* (M), and bare ground control] subjected to heavy (1), moderate (2), or light (3) thinning prior to planting seedlings in the understory. Bars indicate means and error bars the standard error. Different letters in the same month indicate significant differences between treatments ($P < 0.05$). Abbreviations: SLA, specific leaf area; $Chl_{a/b}$, chlorophyll *a* and *b* ratio; $Chl_{total}$, total chlorophyll content; $F_v/F_m$, maximum quantum yield of photosystem II (PSII); Y(II), actual quantum yield of PSII; $A_{sat}$, light-saturated photosynthesis rate; $g_s$, stomatal conductance

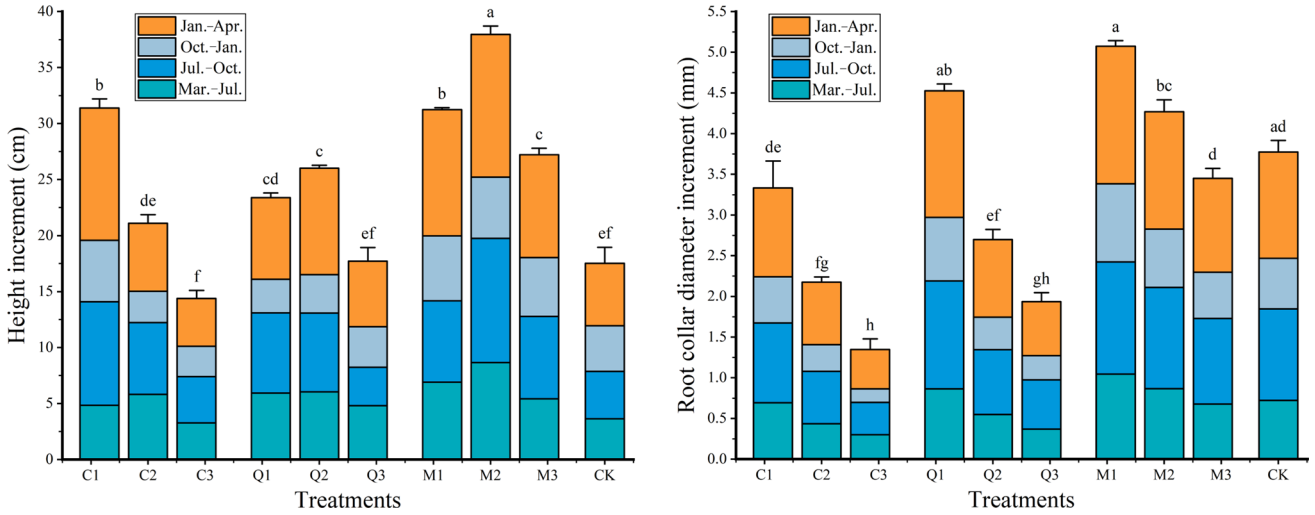


**Fig. 5** Height and root collar diameter increments (March to July 2020, July to October 2020, October to January 2021, January to April 2021) of *P. bournei* seedlings in three stand types [*Cryptomeria japonica* (C), *Quercus acutissima* (Q), mixed forest of *C. japonica* and *Q. acutissima* (M), and bare ground control (CK)] subjected to heavy (1), moderate (2), or light (3) thinning prior to planting; Bars indicate means and error bars the standard error. Different letters in the same month indicate significant differences between treatments ($P < 0.05$)

**Table 3** Effect of thinning levels on the annual relative growth rate (RG) of aboveground biomass and crowns of *P. bournei* seedlings

| Treatments | Crown area ($cm^2$) | | | | RG |
|---|---|---|---|---|---|
| | July 2020 | October 2020 | January 2021 | April 2021 | |
| C1 | $1322.4 \pm 56.9^{abc}$ | $1657.0 \pm 35.4^{a}$ | $1905.9 \pm 29.0^{a}$ | $2303.8 \pm 53.0^{a}$ | $1.31 \pm 0.053^{cd}$ |
| C2 | $1399.6 \pm 23.2^{ab}$ | $1565.1 \pm 44.1^{ab}$ | $1703.3 \pm 62.0^{cd}$ | $1911.3 \pm 44.7^{cd}$ | $0.93 \pm 0.029^{f}$ |
| C3 | $1100.4 \pm 32.0^{cd}$ | $1251.0 \pm 45.4^{cde}$ | $1417.5 \pm 26.9^{fg}$ | $1596.2 \pm 44.1^{fg}$ | $0.65 \pm 0.023^{g}$ |
| Q1 | $1203.0 \pm 10.6^{ac}$ | $1416.4 \pm 35.4^{abc}$ | $1560.7 \pm 39.3^{def}$ | $1789.0 \pm 29.0^{de}$ | $1.45 \pm 0.022^{bc}$ |
| Q2 | $1304.1 \pm 96.0^{abc}$ | $1495.3 \pm 84.1^{abc}$ | $1631.8 \pm 21.5^{cde}$ | $1828.2 \pm 31.7^{de}$ | $1.11 \pm 0.042^{e}$ |
| Q3 | $935.8 \pm 34.8^{e}$ | $1055.7 \pm 42.9^{e}$ | $1172.1 \pm 1.0^{h}$ | $1300.5 \pm 19.2^{h}$ | $0.84 \pm 0.012^{f}$ |
| M1 | $1237.1 \pm 16.6^{abc}$ | $1500.8 \pm 87.2^{abc}$ | $1733.8 \pm 9.5^{bc}$ | $2061.0 \pm 18.0^{bc}$ | $1.64 \pm 0.008^{a}$ |
| M2 | $1453.9 \pm 56.4^{a}$ | $1672.7 \pm 70.7^{a}$ | $1877.4 \pm 37.9^{ab}$ | $2165.6 \pm 28.9^{ab}$ | $1.57 \pm 0.077^{ab}$ |
| M3 | $1136.6 \pm 20.8^{bd}$ | $1325.8 \pm 18.9^{bcd}$ | $1498.1 \pm 17.8^{ef}$ | $1689.9 \pm 18.2^{ef}$ | $1.28 \pm 0.033^{cde}$ |
| CK | $965.9 \pm 64.7^{d}$ | $1130.1 \pm 42.9^{de}$ | $1308.9 \pm 39.3^{gh}$ | $1484.4 \pm 59.0^{g}$ | $1.23 \pm 0.014^{de}$ |

Treatments: stands of *Cryptomeria japonica* (C), *Quercus acutissima* (Q), mixed forest of *C. japonica* and *Q. acutissima* (M), and bare ground control (CK) were subjected to heavy (1), moderate (2), or light (3) thinning prior to planting *P. bournei* seedlings in the understory. Values are means ± standard error; letters in the same month indicate significant differences among treatments ($P < 0.05$)

the development of form and structure affected by light, of plants (Riikonen 2021), with far-red light (long-wave light) also enhancing the photosynthetic efficiency of short-wave light (Emerson et al. 1957; Zhen et al. 2019; Zhen and Bugbee 2020). Consistent with the findings of Ellsworth and Reich (1993) and Zhen et al. (2022) in their studies of the light environment in stands, the proportion of far-red and blue-violet light in the three stands in this study increased as the canopy opening decreased. As seen by the reductions in R/FR and Rw/Bw relative to full sunlight, the spectral composition in the *C. japonica* plantation was affected the most by thinning and the mixed forest was affected the least. After moderate and light thinning, the lower the number of broadleaf trees in the stand, the higher the proportion of far-red and blue-violet light (i.e., the *C. japonica* plantation had the highest proportion of far-red and blue-violet light) (Table 2). Therefore, thinning measures should be targeted according to the species composition of the stand (Wiener 2010) to obtain a stable and healthy canopy structure and a suitable understory environment to help regenerate understory vegetation (particularly key species targeted for regeneration as part of forest management objectives) and to achieve sustainable forest succession (Schwartz et al. 2015; Forrester 2017).

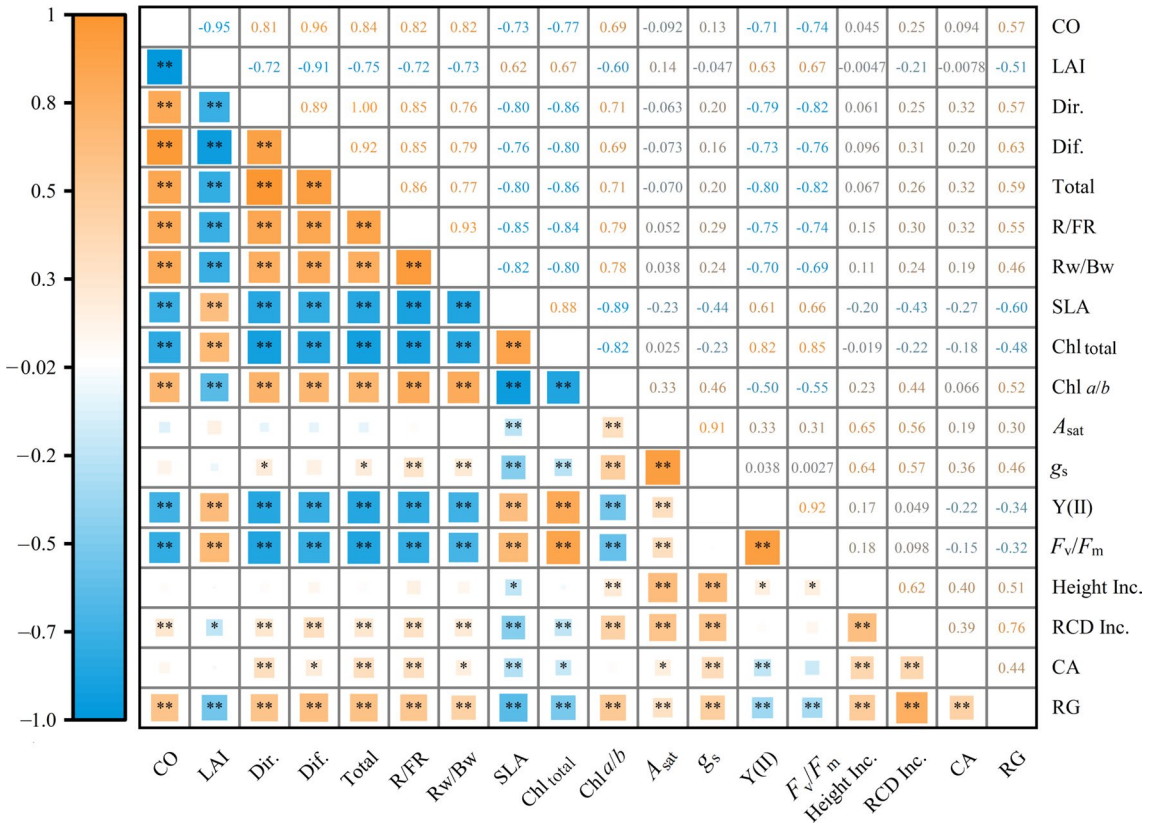


**Fig. 6** Spearman correlation coefficients among stand canopy structure, the understory light environment, and photosynthetic traits and growth of *P. bournei* seedlings (*$P<0.05$; **$P<0.01$). Abbreviations: CO, canopy openness; LAI, leaf area index; CA, crown area; Dir., direct radiation; Dif., diffuse radiation; Total, under-canopy photosynthetic photon flux density including direct and diffuse radiation; R/FR, red radiation/far red radiation ratio; Rw/Bw, wideband red radiation/wideband blue radiation ratio; SLA, specific leaf area; Chl total, total chlorophyll content; $Chl_{a/b}$, chlorophyll *a* and *b* ratio; $A_{sat}$, light-saturated photosynthesis rate; $g_s$, stomatal conductance; Y(II), actual quantum yield of photosystem II (PSII); $F_v/F_m$, maximum quantum yield of PSII; Height Inc, height increments; RCD Inc., root collar diameter increments; CA, crown area; RG, annual relative growth rate of aboveground biomass

### Effects of thinning on photosynthesis and growth of *P. bournei* seedlings in the understory

Light is the most critical factor affecting regeneration and is essential in the survival, growth, and development of seedlings (Dumais et al. 2018; Sendall et al. 2018; Daryaei et al. 2019). *P. bournei*, which is shade-tolerant at a young age and whose light requirements vary with age (An et al. 2022), showed significant different responses to a more heterogeneous light environment relative to those reported in previous studies of pioneer species (shade intolerant species) (Gravel et al. 2010; Zhang et al. 2012; Santos and Ferreira 2020). Several studies have shown that light-induced leaf plasticity is intrinsically linked to the light requirements of plants and therefore, photosynthetic leaf traits are used to predict seedling growth (Poorter and Bongers 2006; Li et al. 2017, 2022). The leaf photosynthetic pathways (light interception, absorption, and use) of *P. bournei* responded quickly and were highly correlated with the understory light environment. In particular, there was a strong intrinsic connection between R/FR and the photosynthetic capacity and growth performance of seedlings (Figs. 4, 6, 7). Studies of plant response to red and far-red light have also found that a slight variation in R/FR can lead to large changes in the phytochrome balance, thus affecting the overall photomorphogenesis of the plant (e.g., photosynthetic leaf traits) (Chelle et al. 2007; Demotes-Mainard et al. 2016).

Photosynthetic leaf traits represent the basic response of plants to changes in the light environment and can be used to predict growth (Santos and Ferreira 2020). Among them, the specific leaf area (SLA) reflects the ability of plant leaves to intercept light and to self-protect under strong light, which is closely related to the growth–survival trade-off of plants (Dahlgren et al. 2006; Kennedy et al. 2007). In this study, the SLA of *P. bournei* seedlings under low light was elevated and the light interception per unit of leaf biomass was increased (Fig. 4a). In addition, because of the increased proportion of far-red and blue light above seedlings under the canopy (Table 2), the $Chl_{total}$ and the percentage of chlorophyll *b* increased (Fig. 4b, c), and their absorption of red

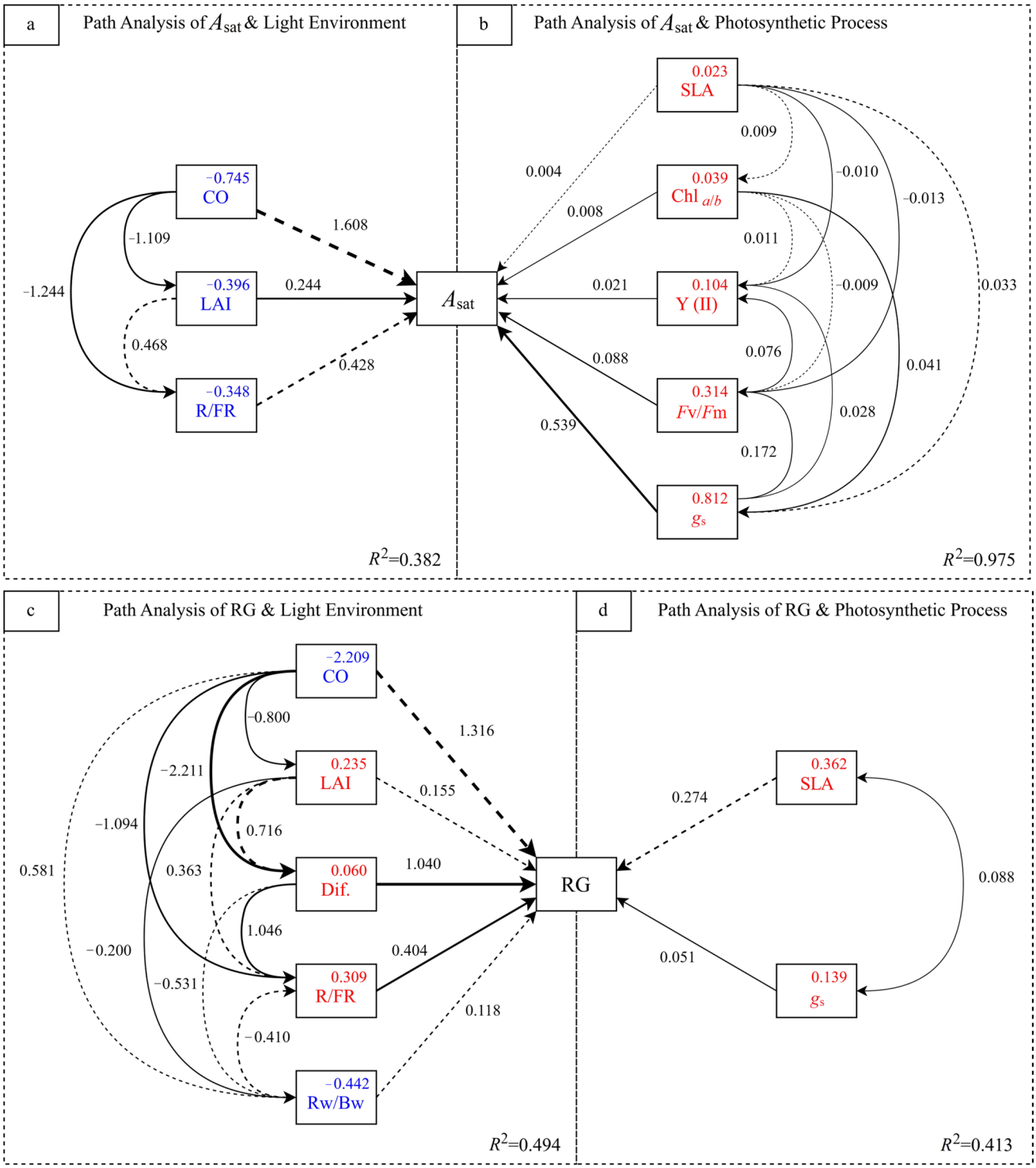


**Fig. 7** Path analysis diagrams showing the direct and indirect effects of relative factors on the light-saturated photosynthesis rate ($A_{sat}$) and the annual relative growth rate (RG) of the aboveground biomass of *P. bournei* seedlings. Only effective paths filtered by stepwise regression analysis are shown in the diagrams. The value beside the arrows indicates the standardized determination coefficient; line thickness indicates the size of the path coefficient, and solid and dash lines the positive and negative path coefficients, respectively. The determination coefficients are shown in the upper right corner of the indicators, and decision and limitation variables are in red and blue, respectively. Abbreviations: CO, canopy openness; LAI, leaf area index; Dif., diffuse radiation; R/FR, red/far red radiation ratio; Rw/Bw, wideband red/wideband blue radiation ratio; SLA, specific leaf area; $Chl_{a/b}$ chlorophyll *a* and *b* ratio; $g_s$, stomatal conductance; Y(II), actual quantum yield of photosystem II (PSII); $F_v/F_m$, maximum quantum yield of PSII

and blue-violet light was enhanced. Finazzi and Johnson (2016) and Zhen et al. (2022) proposed that far-red photons maintain the energy balance between PSII and PSI by enhancing the linear electron transport efficiency and stimulating the cyclic electron flow around PSI, resulting in less photooxidative damage, which may explain how low R/FR enhances the light use of *P. bournei*. Light utilization ability can be effectively reflected by the chlorophyll fluorescence parameters Y(II) and $F_v/F_m$ (Peterson et al. 2001). Immediately after thinning, the Y(II) and $F_v/F_m$ of *P. bournei* seedlings in the shade of a stand showed increased over time with greater shade. However, in the *C. japonica* plantation in which canopies had closed over one year after thinning, the Y(II) of seedlings increased and then decreased as the canopy opening decreased (C3 in Fig. 4d). This suggests that the light resources were severely limited and may have led to stress and reduced light utilization efficiency by *P. bournei*. A direct limiting factor for plant photosynthesis is stomatal conductance ($g_s$) (Santos and Ferreira 2020). In this study, the light environment significantly affected the $g_s$ of *P. bournei* seedlings (Fig. 6) and showed a close internal relationship with $A_{sat}$ and RG (Fig. 7). Similarly, *Schima superba* Gardn. & Champ., which is shade-tolerant as a seedling, responds to rapid changes in the light environment by opening and closing its stomata rapidly (Zhang et al. 2012). Therefore, we hypothesize that a rapid response depending on stomatal opening/closing may also be one of the main mechanisms by which *P. bournei* seedlings adapt to changes in the understory light environment to ensure efficient use of the light resource. The light-saturated photosynthesis rate ($A_{sat}$) characterizes the carbon assimilation rate of plants (De Kauwe et al. 2016). Based on our path analysis of the relationships between the factors (Fig. 7), we hypothesize that the light environment (especially R/FR) indirectly acts on the carbon assimilation rate of plants by directly acting on each step in the photosynthetic pathway of *P. bournei* seedlings, thus affecting their overall growth and development. In addition, the photosynthetic performance of *P. bournei* seedlings grown in full sunlight was inhibited because their leaves had less ability to intercept, absorb, and use light, and lower stomatal conductance and carbon assimilation rates than seedlings grown in shade (Fig. 4). Previous experiments on shade-tolerant tree species such as *Cryptocarya concinna* Hance and *Syzygium acuminatissimum* (Blume) DC cultivated under intense light demonstrated that excess light energy produces toxic products such as superoxide, singlet oxygen, and peroxide which damage the photosynthetic system of plants and limit their growth and development if they are not safely dispersed in a timely manner (Zhang et al. 2012; Roeber et al. 2021).

Plant morphological adjustments to improve the use efficiency of light resources is one of the important strategies that plants use to adapt to environmental changes (Rosati et al. 2013). Crown size is most directly related to light resource acquisition and growth. *P. bournei* seedlings developed smaller crowns under both intense light (controls) and weak light (C3), which reflects their adaptation strategies to both intense and weak light stress. When light is too intense, seedlings reduce their crown area (Zhang et al. 2018c); when light is too weak, access to the resource is insufficient and seedlings reduce crown investment, tolerate the weak light stress, and wait for conditions to improve (Zhang et al. 2012). The light requirements of *P. bournei* are exacting: low light does not meet resource demands and needs to be enhanced to meet light conditions it requires; however, the species is inhibited by high light intensity if it is intentionally increased. Furthermore, its carbon accumulation potential is limited as a shade-tolerant plant; its carbon stocks are small and it faces special risks if it suffers serious light damage (Gravel et al. 2010). Figure 5 shows that the height-to-diameter growth strategy of *P. bournei* seedlings also changed with CO (i.e., the intensity of understory radiation). As light intensity decreased (CK to C3), height-to-diameter ratios increased (4.7–10.7), and seedlings transformed from a diameter growth advantage to a height growth advantage, changing their growth strategy from tolerance to pursuit of light. The findings of the path analysis of factor interactions (Fig. 7) are consistent with the conclusions of Zhang et al. (2018b): the high proportion of far-red light in the understory may act as a 'shade avoidance signal' to make *P. bournei* seedlings sensitive and responsive to shade, and the lower R/FR reduces the proportion of Pfr (far-red light-absorbing form) in the total phytochrome of the plant, inducing a higher level of gibberellin and auxin to promote high growth and the pursuit of light resources. In contrast, intense light may induce an increase in cytokinin and lead to an increased diameters (Demotes-Mainard et al. 2016; Fraser et al. 2016). Therefore, providing a suitable light environment for *P. bournei* during early growth is key to improving its photosynthetic performance and promoting growth and development.

### How to optimize *P. bournei* juvenile planting by regulating light environment

Thinning is an important way to adjust and optimize the light environment of forests (Zhang et al. 2018a). Over the year following the thinning treatments, the best performance of *P. bournei* in terms of growth and development was achieved by gradually transitioning from moderate to heavy thinning in all three stands. Under the same thinning intensity, *P. bournei* in mixed stands performed best possibly because the light availability was greater than in pure coniferous or broadleaf stands. Pretzsch (2014), Forrester (2017) and Forrester et al. (2018) reported similar findings when they studied the canopy structure, light environment and

physiological ecology of mixed and single species stands. The greatest reduction in radiation intensity over time was in the *C. japonica* plantation after thinning. However, the proportion of far-red light in the understory was higher than that in the other stands and induced greater upward growth by the seedlings and thus enabled them to obtain light resources (Zhen et al. 2022). The better early performance of *P. bournei* in the *C. japonica* plantation was also achieved after one year of heavy thinning. However, after heavy thinning of the *Q. acutissima* plantation, *P. bournei* showed intense light suppression; height growth was limited, therefore we suggest that the optimal thinning intensity for a *Q. acutissima* plantation would be between heavy and moderate. Studies by Midgley et al. (2002) and Aiba et al. (2007) indicated that there may be competition for light resource utilization in forests with a mixture of broadleaf species, but the productivity of mixed coniferous and broadleaf forests was higher than that of broadleaf mixed forests.

Based on the best treatment for the growth and development of *P. bournei* saplings in this study, a suitable understory light environment has a photosynthetic photon flux density of 19.1–22.6 mol $m^{-2}$ $d^{-1}$ and a red/far red radiation ratio of 1.0–1.2. Forest managers should not only consider the canopy structure, light conditions, and species composition of stands but also the biological characteristics of species to achieve afforestation targets (Daryaei et al. 2019). A suitable light environment should be created for the understory vegetation and a healthy, stable canopy and stand environment should be established to promote the growth and development of the residual stand (Beaudet et al. 2011; Santos et al. 2020).

## Conclusion

Improvement of the stand light environment by thinning varies, depending on thinning intensity and species composition. Among the three typical stands investigated, the understory light environment of the mixed stand after heavy thinning was the most favorable for the growth of *P. bournei* seedlings, resulting in the largest relative growth. The R/FR ratio is a key light environment factor, regulating the growth and development of *P. bournei*. Photosynthetic leaf traits can predict the early silvicultural benefits of *P. bournei*. Increasing the canopy opening enhances light availability in the understory and improve the light resource use capacity to promote photosynthesis and growth of the seedlings. However, growth is inhibited under intense light. Therefore, afforestation should be combined with sustainable management, avoiding the establishment of *P. bournei* seedlings in full sun, and using *P. bournei* for species restructuring or forest quality improvement. Awareness of forest management goals and of the species that comprise the stand should be undertaken to develop targeted afforestation programs.

**Acknowledgements** We acknowledge the State-owned Zhazuo Forest Farm that supported all fieldwork. We would also like to thank the editor, associate editor, and anonymous reviewers for their helpful feedback and valuable suggestions.



## References

Aiba SI, Hanya G, Tsujino R, Takyu M, Seino T, Kimura K, Kitayama K (2007) Comparative study of additive basal area of conifers in forest ecosystems along elevational gradients. Ecol Res 22(3):439–450. https://doi.org/10.1007/s11284-007-0338-3

An J, Wei XL, Huo HH (2022) Transcriptome analysis reveals the accelerated expression of genes related to photosynthesis and chlorophyll biosynthesis contribution to shade-tolerant in *Phoebe bournei*. BMC Plant Biol 22(1):268. https://doi.org/10.1186/s12870-022-03657-y

Annighöfer P (2018) Stress relief through gap creation? Growth response of a shade tolerant species (*Fagus sylvatica* L.) to a changed light environment. For Ecol Manag 415–416:139–147. https://doi.org/10.1016/j.foreco.2018.02.027

Asanok L, Marod D, Duengkae P, Pranmongkol U, Kurokawa H, Aiba M, Katabuchi M, Nakashizuka T (2013) Relationships between functional traits and the ability of forest tree species to reestablish in secondary forest and enrichment plantations in the uplands of northern Thailand. For Ecol Manag 296:9–23. https://doi.org/10.1016/j.foreco.2013.01.029

Beaudet M, Messier C (2002) Variation in canopy openness and light transmission following selection cutting in northern hardwood stands: an assessment based on hemispherical photographs. Agric For Meteorol 110(3):217–228. https://doi.org/10.1016/S0168-1923(01)00289-1

Beaudet M, Harvey BD, Messier C, Coates KD, Poulin J, Kneeshaw DD, Brais S, Bergeron Y (2011) Managing understory light conditions in boreal mixedwoods through variation in the intensity and spatial pattern of harvest: a modelling approach. For Ecol Manag 261(1):84–94. https://doi.org/10.1016/j.foreco.2010.09.033

Chelle M, Evers JB, Combes D, Varlet-Grancher C, Vos J, Andrieu B (2007) Simulation of the three-dimensional distribution of the red:far-red ratio within crop canopies. New

Phytol 176(1):223–234. https://doi.org/10.1111/j.1469-8137.2007.02161.x
Cogliastro A, Paquette A (2012) Thinning effect on light regime and growth of underplanted red oak and black cherry in post-agricultural forests of south-eastern Canada. New For 43(5–6):941–954. https://doi.org/10.1007/s11056-012-9329-5
Dahlgren JP, Eriksson O, Bolmgren K, Strindell M, Ehrlén J (2006) Specific leaf area as a superior predictor of changes in field layer abundance during forest succession. J Veg Sci 17(5):577–582. https://doi.org/10.1111/j.1654-1103.2006.tb02481.x
Daryaei A, Sohrabi H, Puerta-Piñero C (2019) How does light availability affect the aboveground biomass allocation and leaf morphology of saplings in temperate mixed deciduous forests? New for 50(3):409–422. https://doi.org/10.1007/s11056-018-9666-0
De Kauwe MG, Lin YS, Wright IJ, Medlyn BE, Crous KY, Ellsworth DS, Maire V, Prentice IC, Atkin OK, Rogers A, Niinemets Ü, Serbin SP, Meir P, Uddling J, Togashi HF, Tarvainen L, Weerasinghe LK, Evans BJ, Ishida FY, Domingues TF (2016) A test of the 'one-point method' for estimating maximum carboxylation capacity from field-measured, light-saturated photosynthesis. New Phytol 210(3):1130–1144. https://doi.org/10.1111/nph.13815
Demotes-Mainard S, Péron T, Corot A, Bertheloot J, Le Gourrierec J, Pelleschi-Travier S, Crespel L, Morel P, Huché-Thélier L, Boumaza R, Vian A, Guérin V, Leduc N, Sakr S (2016) Plant responses to red and far-red lights, applications in horticulture. Environ Exp Bot 121:4–21. https://doi.org/10.1016/j.envexpbot.2015.05.010
Dumais D, Larouche C, Raymond P, Bédard S, Lambert MC (2018) Survival and growth dynamics of red spruce seedlings planted under different forest cover densities and types. New For 50(4):573–592. https://doi.org/10.1007/s11056-018-9680-2
Ellsworth DS, Reich PB (1993) Canopy structure and vertical patterns of photosynthesis and related leaf traits in a deciduous forest. Oecologia 96(2):169–178. https://doi.org/10.1007/bf00317729
Emerson R, Chalmers R, Cederstrand C (1957) Some factors influencing the long-wave limit of photosynthesis. PNAS 43(1):133–143. https://doi.org/10.1073/pnas.43.1.133
Finazzi G, Johnson GN (2016) Cyclic electron flow: facts and hypotheses. Photosynth Res 129(3):227–230. https://doi.org/10.1007/s11120-016-0306-2
Forrester DI (2017) Ecological and physiological processes in mixed versus monospecific stands. In: Pretzsch H, Forrester DI, Bauhus J (eds) Mixed-species forests. Springer, Berlin, pp 73–115
Forrester DI, Ammer C, Annighöfer PJ, Barbeito I, Bielak K, Bravo-Oviedo A, Coll L, Río MD, Drössler L, Heym M, Hurt V, Löf M, Ouden JD, Pach M, Pereira MG, Plaga BNE, Ponette Q, Skrzyszewski J, Sterba H, Svoboda M, Zlatanov TM, Pretzsch H (2018) Effects of crown architecture and stand structure on light absorption in mixed and monospecific *Fagus sylvatica* and *Pinus sylvestris* forests along a productivity and climate gradient through Europe. J Ecol 106(2):746–760. https://doi.org/10.1111/1365-2745.12803
Fraser DP, Hayes S, Franklin KA (2016) Photoreceptor crosstalk in shade avoidance. Curr Opin Plant Biol 33:1–7. https://doi.org/10.1016/j.pbi.2016.03.008
Ge YJ, He XY, Wang JF, Jiang B, Ye RH, Lin XC (2014) Physiological and biochemical responses of *Phoebe bournei* seedlings to water stress and recovery. Acta Physiol Plant 36(5):1241–1250. https://doi.org/10.1007/s11738-014-1502-3
Giertych MJ, Karolewski P, Oleksyn J (2015) Carbon allocation in seedlings of deciduous tree species depends on their shade tolerance. Acta Physiol Plant 37(10):216. https://doi.org/10.1007/s11738-015-1965-x
Gravel D, Canham CD, Beaudet M, Messier C (2010) Shade tolerance, canopy gaps and mechanisms of coexistence of forest trees. Oikos 119(3):475–484. https://doi.org/10.1111/j.1600-0706.2009.17441.x
Gustafsson M, Gustafsson L, Alloysius D, Falck J, Yap S, Karlsson A, Ilstedt U (2016) Tree traits and canopy closure data from an experiment with 34 planted species native to Sabah, Borneo. Data Brief 6:466–470. https://doi.org/10.1016/j.dib.2015.12.048
He PC, Wright IJ, Zhu SD, Onoda Y, Liu H, Li RH, Liu XR, Hua L, Oyanoghafo OO, Ye Q (2019) Leaf mechanical strength and photosynthetic capacity vary independently across 57 subtropical forest species with contrasting light requirements. New Phytol 223(2):607–618. https://doi.org/10.1111/nph.15803
Ishii HT, Tanabe SI, Hiura T (2004) Exploring the relationships among canopy structure, stand productivity, and biodiversity of temperate forest ecosystems. For Sci 50(3):342–355. https://doi.org/10.1093/forestscience/50.3.342
Kennedy S, Black K, O'Reilly C, Ní Dhubháin Á (2007) The impact of shade on morphology, growth and biomass allocation in *Picea sitchensis*, *Larix* × *eurolepis* and *Thuja plicata*. New for 33(2):139–153. https://doi.org/10.1007/s11056-006-9019-2
Kohyama T, Hotta M (1990) Significance of allometry in tropical saplings. Funct Ecol 4(4):515–521. https://doi.org/10.2307/2389319
Li Y, Krober W, Bruelheide H, Hardtle W, von Oheimb G (2017) Crown and leaf traits as predictors of subtropical tree sapling growth rates. J Plant Ecol 10(1):136–145. https://doi.org/10.1093/jpe/rtw041
Li XN, Wang YH, Yang ZH, Liu T, Mu CC (2022) Photosynthesis adaption in Korean pine to gap size and position within *Populus davidiana* forests in Xiaoxing'anling. China J For Res 33(5):1517–1527. https://doi.org/10.1007/s11676-021-01439-0
Lichtenthaler HK, Wellburn AR (1983) Determinations of total carotenoids and chlorophylls a and b of leaf extracts in different solvents. Biochem Soc Trans 11(5):591–603. https://doi.org/10.1042/bst0110591
Lochhead KD, Comeau PG (2012) Relationships between forest structure, understory light and regeneration in complex Douglas-fir dominated stands in south-eastern British Columbia. For Ecol Manag 284:12–22. https://doi.org/10.1016/j.foreco.2012.07.029
Matsuo T, Martinez-Ramos M, Bongers F, van der Sande MT, Poorter L (2021) Forest structure drives changes in light heterogeneity during tropical secondary forest succession. J Ecol 109(8):2871–2884. https://doi.org/10.1111/1365-2745.13680
Midgley JJ, Parker R, Laurie H, Seydack A (2002) Competition among canopy trees in indigenous forests: an analysis of the 'additive basal area' phenomenon. Austral Ecol 27(3):269–272. https://doi.org/10.1046/j.1442-9993.2002.01177.x
Niinemets U (2010) A review of light interception in plant stands from leaf to canopy in different plant functional types and in species with varying shade tolerance. Ecol Res 25(4):693–714. https://doi.org/10.1007/s11284-010-0712-4
Oguchi R, Hikosaka K, Hiura T, Hirose T (2006) Leaf anatomy and light acclimation in woody seedlings after gap formation in a cool-temperate deciduous forest. Oecologia 149(4):571–582. https://doi.org/10.1007/s00442-006-0485-1
Orman O, Wrzesinski P, Dobrowolska D, Szewczyk J (2021) Regeneration growth and crown architecture of European beech and silver fir depend on gap characteristics and light gradient in the mixed montane old-growth stands. For Ecol Manag 482:118866. https://doi.org/10.1016/j.foreco.2020.118866
Peterson RB, Oja V, Laisk A (2001) Chlorophyll fluorescence at 680 and 730 nm and leaf photosynthesis. Photosynth Res 70(2):185–196. https://doi.org/10.1023/a:1017952500015
Poorter L, Bongers F (2006) Leaf traits are good predictors of plant performance across 53 rain forest species. Ecology 87(7):1733–1743. https://doi.org/10.1890/0012-9658(2006)87[1733:Ltagpo]2.0.Co;2

Pretzsch H (2014) Canopy space filling and tree crown morphology in mixed-species stands compared with monocultures. For Ecol Manag 327:251–264. https://doi.org/10.1016/j.foreco.2014.04.027

Riikonen J (2021) Applications of different light spectra in growing forest tree seedlings. Forests 12(9):4. https://doi.org/10.3390/f12091194

Roeber VM, Bajaj I, Rohde M, Schmulling T, Cortleven A (2021) Light acts as a stressor and influences abiotic and biotic stress responses in plants. Plant Cell Environ 44(3):645–664. https://doi.org/10.1111/pce.13948

Rosati A, Paoletti A, Caporali S, Perri E (2013) The role of tree architecture in super high density olive orchards. Sci Hortic 161:24–29. https://doi.org/10.1016/j.scienta.2013.06.044

Santos VAHF, Ferreira MJ (2020) Are photosynthetic leaf traits related to the first-year growth of tropical tree seedlings? A light-induced plasticity test in a secondary forest enrichment planting. For Ecol Manag 460:117900. https://doi.org/10.1016/j.foreco.2020.117900

Santos V, Nelson BW, Rodrigues J, Garcia MN, Ceron JVB, Ferreira MJ (2019) Fluorescence parameters among leaf photosynthesis-related traits are the best proxies for $CO_2$ assimilation in Central Amazon trees. Braz J Bot 42(2):239–247. https://doi.org/10.1007/s40415-019-00533-2

Santos VAHF, Modolo GS, Ferreira MJ (2020) How do silvicultural treatments alter the microclimate in a Central Amazon secondary forest? A focus on light changes. J Environ Manag 254:109816. https://doi.org/10.1016/j.jenvman.2019.109816

Schwartz G, Ferreira MS, Lopes JC (2015) Silvicultural intensification and agroforestry systems in secondary tropical forests: a review. Amaz J Agric Environ Sci 58(3):319–326. https://doi.org/10.4322/rca.1830

Sendall KM, Reich PB, Lusk CH (2018) Size-related shifts in carbon gain and growth responses to light differ among rainforest evergreens of contrasting shade tolerance. Oecologia 187(3):609–623. https://doi.org/10.1007/s00442-018-4125-3

Silveira LCI, Brasileiro BP, Kist V, Weber H, Daros E, Peternelli LA, Barbosa MHP (2015) Selection strategy in families of energy cane based on biomass production and quality traits. Euphytica 204(2):443–455. https://doi.org/10.1007/s10681-015-1364-9

Strasser RJ, Tsimilli-Michael M, Qiang S, Goltsev V (2010) Simultaneous in vivo recording of prompt and delayed fluorescence and 820 nm reflection changes during drying and after rehydration of the resurrection plant *Haberlea rhodopensis*. Biochim Biophys Acta Bioenerg 1797:122–122. https://doi.org/10.1016/j.bbabio.2010.04.365

Tsimilli-Michael M, Strasser RJ (2008) In vivo assessment of stress impact on plant's vitality: applications in detecting and evaluating the beneficial role of mycorrhization on host plants. In: Varma A (ed) Mycorrhiza. Springer, Berlin, pp 679–703

Wang HY, Wu F, Li M, Liang DQ, Ding GJ (2021a) Heteroblastic foliage affects the accumulation of non-structural carbohydrates and biomass in *Pinus massoniana* (Lamb.) seedlings. Forests 12(12):16. https://doi.org/10.3390/f12121686

Wang X, Wei XL, Wu GY, Chen SQ (2021b) Ammonium application mitigates the effects of elevated carbon dioxide on the carbon/nitrogen balance of *Phoebe bournei* seedlings. Tree Physiol 41(9):1658–1668. https://doi.org/10.1093/treephys/tpab026

Wei HX, Chen X, Chen GS, Zhao HT (2019) Foliar nutrient and carbohydrate in Aralia elata can be modified by understory light quality in forests with different structures at Northeast China. Ann For Res 62(2):125–137. https://doi.org/10.15287/afr.2019.1395

Wiener EM (2010) Ecological research and the management of young successional forests: a case study on the reintroduction of native tree species on a *Terra Firme* site in northeastern Peru. J Sustain Forest 29(6–8):571–590. https://doi.org/10.1080/10549811003739098

Zha MQ, Han YZ, Cheng XR (2022) Mixing planting proportions in a plantation affects functional traits and biomass allocation of *Cunninghamia lanceolata* and *Phoebe bournei* seedlings. J For Res 33(6):1793–1805. https://doi.org/10.1007/s11676-022-01464-7

Zhang Q, Chen YJ, Song LY, Liu N, Sun LL, Peng CL (2012) Utilization of lightflecks by seedlings of five dominant tree species of different subtropical forest successional stages under low-light growth conditions. Tree Physiol 32(5):545–553. https://doi.org/10.1093/treephys/tps043

Zhang T, Dong XB, Guan HW, Meng Y, Ruan JF, Wang ZY (2018a) Effect of thinning on the spatial structure of a *Larix gmelinii* Rupr. secondary forest in the Greater Khingan Mountains. Forests 9(11):720. https://doi.org/10.3390/f9110720

Zhang T, Yan QL, Wang J, Zhu JJ (2018b) Restoring temperate secondary forests by promoting sprout regeneration: effects of gap size and within-gap position on the photosynthesis and growth of stump sprouts with contrasting shade tolerance. For Ecol Manag 429:267–277. https://doi.org/10.1016/j.foreco.2018.07.025

Zhang TJ, Zheng J, Yu ZC, Gu XQ, Tian XS, Peng CL, Chow WS (2018c) Variations in photoprotective potential along gradients of leaf development and plant succession in subtropical forests under contrasting irradiances. Environ Exp Bot 154:23–32. https://doi.org/10.1016/j.envexpbot.2017.07.016

Zhen SY, Bugbee B (2020) Far-red photons have equivalent efficiency to traditional photosynthetic photons: implications for redefining photosynthetically active radiation. Plant Cell Environ 43(5):1259–1272. https://doi.org/10.1111/pce.13730

Zhen SY, Haidekker M, van Iersel MW (2019) Far-red light enhances photochemical efficiency in a wavelength-dependent manner. Physiol Plant 167(1):21–33. https://doi.org/10.1111/ppl.12834

Zhen SY, van Iersel MW, Bugbee B (2022) Photosynthesis in sun and shade: the surprising importance of far-red photons. New Phytol 236(2):538–546. https://doi.org/10.1111/nph.18375